International Journal of Engineering Research & Technology (IJERT)
ISSN: 2278-0181
Vol. 2 Issue 12, December - 2013

Comparative Study Between (CSI based STATCOM and VSI based STATCOM) Used For Current Unbalance Compensation

Anas Benslimane
Laboratory of Electrical Engineering and Maintenance
Higher School of Technology
Oujda, Morocco

Jamal Bouchnaif
Laboratory of Electrical Engineering and Maintenance
Higher School of Technology
Oujda, Morocco

Mohamed Azizi
Laboratory of Electrical Engineering and Maintenance
Higher School of Technology
Oujda, Morocco

Abstract

The sub-stations of the high speed railway connected to the high voltage power system, are considered pollutant loads, and disrupting power grid. The major problem of these sub-stations is the current unbalance caused by the connection between two phases of high voltage power grid. In general case, the shunt STATCOMs used for current unbalanced compensation, are based on voltage source inverter (VSI). By using a current source inverter (CSI) we obtain important performances compared to the VSI structure.

In this paper, we presented a comparative study between the two structures of shunt STATCOM (VSI and CSI), in order to evaluate the current unbalance compensation performances and the sizing optimization.

IJERT

1. Introduction

A large DC inductor and a current control system, allow the CSI_STATCOM to offer very interesting performances. CSI topology offers a number of distinct advantages below compared to VSI, [1]:

- Inverter power circuit size reduction;
- Direct control of the injected current;
- No risk of DC link source short-circuit, because it is a current source realized by an inductor;
- High converter reliability, due to the unidirectional nature of the switches.

The DC link inductor must be equipped by a protection circuit against overvoltage caused by the circuit opening [6]. This work shows that the current source inverter-based STATCOM (CSI) can be exploited to compensate the current unbalance with optimal sizing of the power circuit, on the other side the compensation performance are lower compared to of the voltage source inverter-based STATCOM (**VSI**). The classic structure of VSI_STATCOM used for unbalanced compensation is explained in the first part of this paper. Then, the power circuit and the current control loop for shunt CSI_STATCOM is studied. Finally, this study is applied to the future sub-station for a new high speed railway (**HSR**) in Morocco, and the model for each structure is simulated in MATLAB/Simulink environment.

2. Current unbalance caused by the high speed railway sub-stations

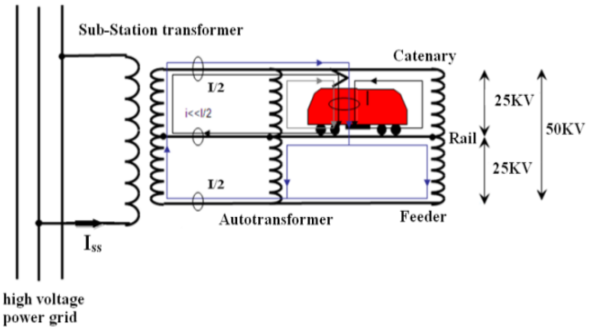

“**Figure 1:** The electrification system of high speed railway (2*25KV-50Hz)”

Usually, the single-phase transformer in a HSR sub-station is connected to two phases of high voltage power grid (Figure 1). In this case, the symmetrical components of current and current unbalance factor Ti obtained by the Fortescue transformation are as follows [2],[7]:

$$\begin{cases} I_1 = I_{ss} \\ I_2 = -I_{ss} \\ I_3 = 0 \end{cases} = F \Rightarrow \begin{cases} I_d = \frac{\sqrt{3}}{3} I_{ss}.e^{-j\frac{\pi}{6}} \\ I_i = \frac{\sqrt{3}}{3} I_{ss}.e^{j\frac{\pi}{6}} \quad \text{and } T_i = \frac{|I_i|}{|I_d|} = 100\% \\ I_o = 0 \end{cases} \quad \textbf{(1)}$$

With:

I_{ss}: current consumed by the substation;

I_i, I_d, I_o : symmetrical components of three-phase current, respectively negative, positive, and zero-sequence;

F: Fortescue transformation matrix;

With:

$$F = \frac{1}{3}\begin{bmatrix} 1 & 1 & 1 \\ 1 & a & a^2 \\ 1 & a^2 & a \end{bmatrix} \text{ and } a = e^{j\frac{2\pi}{3}} \qquad \textbf{(2)}$$

Note that the negative sequence of the current is very large, which generates unbalanced voltages at different points in the network. The shunt STATCOM used to compensate this unbalance is equivalent to an AC current source. It injects at the connection point the negative sequence current **I_i**, in order to control the current unbalance factor **Ti** to a value **2%** limited by the standards [2].

3. Classical structure of VSI_STATCOM

The voltage structure of shunt STATCOM (Figure 2) is composed of a PWM voltage source inverter, a current filtering inductor **L'** (with an internal resistance **R'**), a coupling transformer with ratio (**m**), and an energy storage circuit often capacitive which represents a DC voltage source (**V_{dc}**)[2].

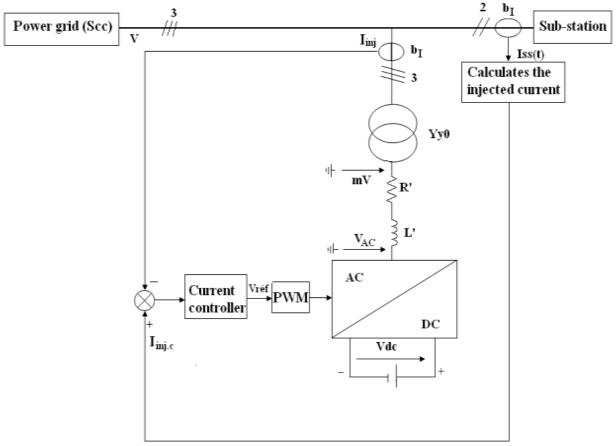

"**Figure 2:** Classical structure of VSI_STATCOM"

3.1. Power circuit of VSI_STATCOM

The injected current rms value **I_{inj}** depends on the current sub-station [2]:

$$|I_{inj}| = |I_i| = \frac{\sqrt{3}}{3}|I_{ss}| \qquad \textbf{(3)}$$

With:

|X|: Rms value (with X is a voltage or current);

The Inductor (**L'**) is calculated by using the equation below [2]:

$$L' \geq \frac{100.m.V_{dc}}{\sqrt{2}.12.f_d.\delta I_{inj}(\%).|I_{inj}|_{min}} \qquad \textbf{(4)}$$

With:

f_d: Carrier frequency of the PWM control;

$\delta I_{inj}(\%)$: Injected current ripple;

The DC side voltage **V_{dc}** is calculated according to the maximum magnitude between the three phase-ground voltages AC side of inverter (**V_{AC1}, V_{AC2}, V_{AC3}**), because these voltages are unbalanced [2]. For a voltage source inverter with PWM control, **V_{dc}** equal:

$$V_{dc} = 2.\sqrt{2}.\max\{|V_{AC1}|, |V_{AC2}|, |V_{AC3}|\} \qquad \textbf{(5)}$$

In the phase number i, we have:

$$|V_{ACi}| = \left| mV_i + (R' + jL'\omega_r)\frac{1}{m} I_{inj,i} \right| \qquad \textbf{(6)}$$

With:

V_i: Phase-to-ground voltage at the connection point to the power grid;

ω_r: Pulsation of the power grid voltage (**$\omega_r = 2.\pi.f_r$**);

The **V_{dc}** voltage must be maintained at a constant value, using one of both following techniques:

- Additions of a voltage control loop of **V_{dc}** in the inverter control;
- The state feedback control of VSI_STATCOM, with **V_{dc}** is a state variable of the system.

The power switches for a voltage source inverter must support a voltage **V_{sw}** and a current **I_{sw}** [3]:

$$I_{sw} \geq \sqrt{2}*(1/m)*|I_{inj}| \quad \text{and} \quad V_{sw} \geq V_{dc} \qquad \textbf{(7)}$$

3.2. Injected current control in the VSI topology

IJERT

The principle of this control (Figure 3) is to find the current to be injected using the sub-station current $\mathbf{I_{ss}}$ [2]:

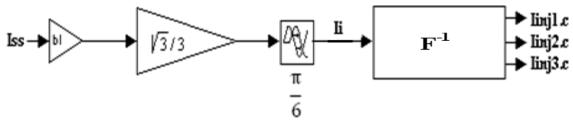

“**Figure 3:** Calculation technique of currents to be injected.”

With:

$\mathbf{b_I}$ **:** Gain of the current sensor;
$\mathbf{I_{inj.c}}$ **:** Currents to be injected;
$\mathbf{F^{-1}}$**:** Fortescue inverse transformation matrix.

The current controller is a proportional integral with the transfer function:

$$R_i^{|}(p) = K^{|}.\frac{1+(\tau_I^{|}.p)}{\tau_I^{|}.p}$$

(8)

The injected current control loop for VSI_STATCOM is below:

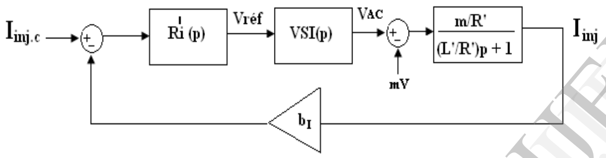

“**Figure 4:** Structure of the current control loop.”

With:

$$\mathbf{VSI(p)} = \frac{\frac{V_{dc}}{2}}{V_{pmax}}$$: Transfer function of the VSI;

$$\frac{\frac{m}{R'}}{1+(\frac{L'}{R'}.p)}$$: Transfer function of (filtering inductor + coupling transformer);

$\mathbf{V_{pmax}}$ **:** Magnitude of the PWM carrier;
$\mathbf{V_{réf}}$**:** The sinusoidal reference of PWM voltage source inverter;

The time constant of the PI controller is maintained to the value (**τ_I’=L’/R’**), so the expression of the closed loop transfer function of the system is

$$T_{BF}(p) = \frac{1}{b_I}\cdot\frac{1}{1+\frac{\tau_I^{|}}{b_I.K'.G'}.p} \qquad \textbf{(9)}$$

With: $$G' = \frac{m.\frac{V_{dc}}{2}}{R'.V_{p\max}}$$

The response time of the system is:

$$T_r = \frac{3.\tau_I^{|}}{b_I.K'.G'} \qquad \textbf{(10)}$$

K’ is given by the expression below using the response time $\mathbf{T_r}$:

$$\mathbf{K' = \frac{3.\tau_I^{|}}{b_I.T_r.G'}} \qquad \textbf{(11)}$$

4. General structure of CSI_STATCOM

The current structure of the shunt STATCOM (Figure 5) is composed of, a PWM current source inverter, a second order filter (**RLC**), a coupling transformer with the same characteristic of the VSI_STATCOM, and a DC current source $\mathbf{I_{dc}}$ often made by an inductive energy storage circuit [4].

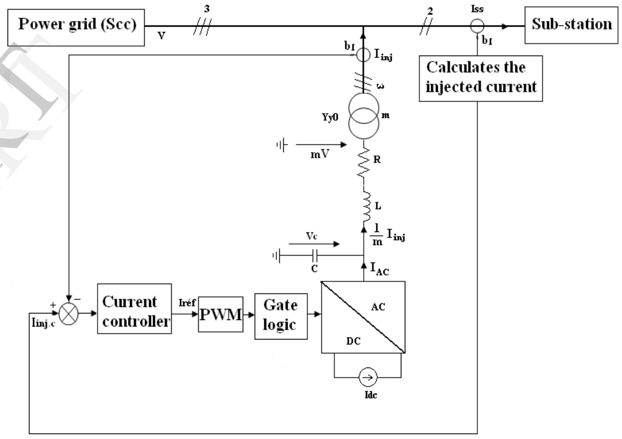

“**Figure 5:** General structure of CSI_STATCOM.”

4.1. Power circuit of CSI_STATCOM

The rms value of the injected current is the same as the VSI structure (Equation 3).

4.1.1 RLC filter

The (Figure 6) , presents the single-phase schema of second order filter (**RLC**) between the coupling transformer secondary and AC side of the current source inverter.

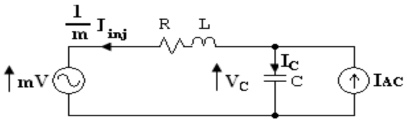

“**Figure 6:** Single-phase schema of RLC filter.”

IJERT IJERT

With:

I_{AC}: AC side current of the CSI;

V_c, I_c: Respectively voltage and current in the filter capacitor;

(1/m)I_{inj}: Injected current at the coupling transformer secondary.

The transfer function of the **RLC** filter is as follows:

$$F(p)=\frac{\frac{1}{m}I_{inj}(p)}{I_{AC}(p)-CpmV(p)}=\frac{m}{(1+\frac{2\xi}{\omega_0}\cdot p+\frac{1}{\omega_0^2}\cdot p^2)} \quad \textbf{(12)}$$

With:

$$LC=\frac{1}{\omega_0^2} \quad \text{And} \quad RC=\frac{2\xi}{\omega_0}$$

ω_0: Natural pulsation of the **RLC** filter;

ξ: Damping factor of the **RLC** filter.

This filter introduces the **LC** oscillations with a low damping factor, because the value of **R** is small. These oscillations disrupt the system stability. For this reason, the natural pulsation should be superior to the network voltage pulsation (**$\omega_0>\omega_r$**) [4].

4.1.2 Sizing the CSI power switches

The switches characteristics are obtained using the DC current **I_{dc}**, and the capacitor voltage **V_C**. In the case of PWM current source inverter, the DC current **I_{dc}** is linked to the fundamental rms value of inverter AC side current |**I_{AC}**|, by the following equation [3]:

$$I_{dc}=\sqrt{2}.|I_{AC}| \quad \textbf{(13)}$$

We assume that the voltages at the power grid connection point are balanced with positive sequence. The injected currents are balanced with negative sequence. We take **V_1** as reference phases. By applying the Fortescue transformation on the power grid voltages and injected currents; the following symmetrical components are obtained:

$$\begin{cases} V_d=V_1 \\ V_i=0 \\ V_O=0 \end{cases} \quad \text{And} \quad \begin{cases} I_{inj,d}=0 \\ I_{inj,i}=I_{inj,1}=I_i \\ I_{inj,o}=0 \end{cases} \quad \textbf{(14)}$$

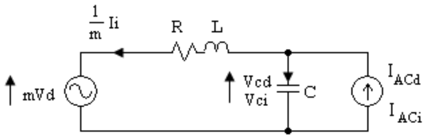

“**Figure 7:** Symmetrical components of CSI_STATCOM.”

With:

X_i,X_d,X_o : Symmetrical components of X, respectively negative, positive, and zero-sequence (with X is a three-phases voltages or three-phases currents);

If the AC side current harmonics are neglected relative to the fundamental, the symmetrical components of **V_C** voltages and **I_{AC}** currents are:

$$\begin{cases} V_{Cd}=mV_d \\ V_{Ci}=\frac{1}{m}.I_i.Z_{RL} \\ V_{CO}=0 \end{cases} \quad \text{And} \quad \begin{cases} I_{ACd}=\frac{V_{Cd}}{Z_C} \\ I_{ACi}=\frac{V_{Ci}}{Z_C}+\frac{1}{m}.I_i \\ I_{ACo}=0 \end{cases} \quad \textbf{(15)}$$

With **Z_{RL}** and **Z_C** are the **RLC** filter impedances:

$$\begin{cases} Z_{RL}=\sqrt{R^2+(L\omega_r)^2}.e^{-jArc\tan(\frac{L\omega_r}{R})} \\ Z_C=\frac{1}{C.\omega_r}e^{j\frac{\pi}{2}} \end{cases} \quad \textbf{(16)}$$

Note that the currents **I_{AC}** and the voltages **V_C** in the inverter output contain an additional component, which means that they are unbalanced. The DC link current **I_{dc}** must be calculated according to the maximum rms value between the three currents **I_{AC}**. IAC are given by the Fortescue inverse transformation:

$$\begin{cases} I_{ACd}=\frac{V_{Cd}}{Z_C} \\ I_{ACi}=\frac{V_{Ci}}{Z_C}+\frac{1}{m}I_i \\ I_{ACo}=0 \end{cases} == F^{-1} ==> \begin{cases} I_{AC1}=I_{ACd}+I_{ACi} \\ I_{AC2}=a^2.I_{ACd}+a.I_{ACi} \\ I_{AC3}=a.I_{ACd}+a^2.I_{ACi} \end{cases} \quad \textbf{(17)}$$

So :

$$\mathbf{I_{dc}=\sqrt{2}*max\ \{|I_{AC1}|,\ |I_{AC2}|,\ I_{AC3}|\}} \quad \textbf{(18)}$$

The DC current source **I_{dc}** is generally made by an inductive circuit (**L_{dc}**) with an internal resistance (**R_{dc}**). The **I_{dc}** average current must be maintained at a constant value. Regulation of this average current in the energy storage inductor is obtained

IJERT

by using the equation of active power balance between the inverter DC side and the power grid AC side [4], or by the state feedback control, in which $\mathbf{I_{dc}}$ is one of the system state variables [5].

The three-phase voltages $\mathbf{V_C}$ across **C** are given in functions of their symmetrical components:

$$\begin{cases} V_{Cd} = mV_d \\ V_{Ci} = \dfrac{1}{m} I_i.Z_{RL} == F^{-1} ==> \\ V_{Co} = 0 \end{cases} \begin{cases} V_{C1} = V_{Cd} + V_{Ci} \\ V_{C2} = a^2.V_{Cd} + a.V_{Ci} \\ V_{C3} = a.V_{Cd} + a^2.V_{Ci} \end{cases} \quad \mathbf{(19)}$$

The power switches for a current source inverter must support a voltage $\mathbf{V_{sw}}$ and a current $\mathbf{I_{sw}}$ [3]:

$$\mathbf{I_{sw} \geq I_{dc}} \text{ and } \mathbf{V_{sw} \geq \sqrt{2}*max\ \{|V_{C1}|, |V_{C2}|, |V_{C3}|\}} \quad \mathbf{(20)}$$

4.2 Injected current control in the CSI topology

The injected current set-point in the phases is the same as for VSI_STATCOM. The current control loop imposes the instantaneous value of the injected current. The choice of the current controller is according to the regulation objectives and the output filter order.

4.2.1 Modelling the PWM current source inverter

The PWM carrier frequency is greater than network frequency ($\mathbf{f_d >> f_r}$). This allows to neglect the first six harmonics in comparison to the current fundamental ($\mathbf{I_{AC}}$) of the inverter. The CSI introduces a phase shift of $\boldsymbol{\pi/6}$ between the sinusoidal reference of PWM block ($\mathbf{I_{ref}}$) and the AC side current fundamental ($\mathbf{I_{AC}}$):

$$I_{réf}(t) = \sin(\omega_r t) \rightarrow PWM\_CSI \rightarrow I_{AC}(t) = \frac{I_{dc}}{V_{pmax}} \sin(\omega_r t + \frac{\pi}{6}) \quad \mathbf{(21)}$$

The transfer function of this inverter is given by the following equation:

$$CSI(p) = \frac{I_{AC}(p)}{I_{réf}(p)} = \frac{\sqrt{3}}{2} \frac{I_{dc}}{V_{pmax}} (1 + \frac{1}{\sqrt{3}.\omega_r} p) \quad \mathbf{(22)}$$

A delay time that corresponds to carrier period ($\mathbf{T_d = 1/f_d}$) is introduced, so:

$$\mathbf{CSI(p) = \frac{\sqrt{3}}{2} \frac{I_{dc}}{V_{pmax}} \frac{(1 + \frac{1}{\sqrt{3}.\omega_r} p)}{(1 + T_d p)}} \quad \mathbf{(23)}$$

4.2.2 Choice of injected current controller

From the equation (12) and (23), the structure of the injected current control loop is given below:

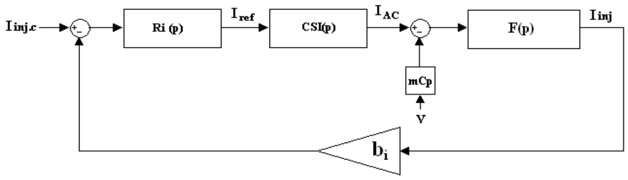

“**Figure 8:** Structure of the injected current control loop”

The transfer function of the CSI_STATCOM direct chain without controller ($\mathbf{R_i(p)=1}$) is:

$$T_D(p) = \frac{\sqrt{3}}{2} \cdot m \cdot \frac{I_{dc}}{V_{pmax}} \cdot \frac{(1 + \frac{1}{\sqrt{3}.\omega_r} p)}{(1 + T_d p)} \cdot \frac{1}{LCp^2 + RCp + 1} \quad \mathbf{(24)}$$

To compensate the phase shift introduced by the current source inverter and to improve the control performances. A controller composed of a mixed PID multiplied by a phase delay controller is proposed.

IJERT

$$\mathbf{R_i(p) = K_p \cdot \frac{1 + \tau p}{1 + (r.\tau p)} \cdot \frac{1 + \tau_I p + (\tau_I.\tau_d) p^2}{\tau_I p}} \quad \mathbf{(25)}$$

With:

$$\mathbf{\tau_I.\tau_d = LC;\ \tau_I = RC;\ \tau = T_d,\ r=3} \quad \mathbf{(26)}$$

$\mathbf{K_p}$ is increased to have an optimal response time.

5. Comparative study and simulation

To evaluate the possibilities of the unbalance compensation, in cost viewpoint, we must compare the voltage and current values supported by each switch for both structures (VSI and CSI). We must compare the current unbalance factor **Ti(%)** and total harmonic current distortion **THD(%)** obtained by both structures, in order to evaluate the unbalance compensation quality.

This study is applied to the future sub-station expected for the high speed railway Tangier-Kenitra in Morocco.

This sub-station has the following electrical characteristics:

- Nominal apparent power $\mathbf{S_{ss,n} = 60MVA}$;
- Reactive power compensated **cosφ≈1**;
- Connection between two phases on a **225KV** power grid;
- The short-circuit power at the connection point equal $\mathbf{S_{cc} = 800MVA}$.

High voltage power grid which supplies this sub-station has the following electrical characteristics:

- The limit of the voltage harmonic level is **5%**;
- The limit of the voltage unbalance factor is **2%**;
- The characteristics of the power grid line are :

$$R_{line}(\Omega/Km)=0.129;\ L_{line}(mH/Km)=1.366;\ C_{line}(nF/Km)=9.1$$

The variation of the apparent power consumed by the sub-station depends on the high speed train traffic movement. The mean value of the apparent power consumed by the sub-station is presented in Figure (9). This mean value is calculated for **10min** period:

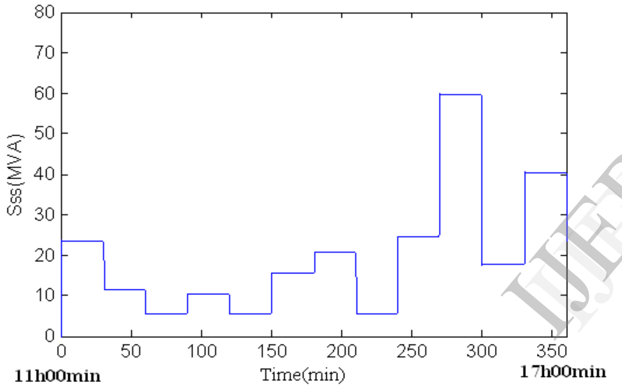

"**Figure 9:** Sub-station apparent power for a daily railway traffic."

The sizing of the CSI and VSI power circuit is based on the sub-station nominal apparent power. The rms value of the nominal injected current is $|I_{inj}|=154A$.

For both structures (CSI and VSI):

- PWM carrier frequency $f_d = 10Khz$;
- Coupling transformer ratio **m=0.1**;
- Current sensor gain $b_i=4.6*10^{-3}\ V/A$;

5.1 Sizing CSI_STATCOM parameters

The natural pulsation of the output filter is $\omega_0=3.5*\omega_r=2.\pi.f_r=1099{,}56\ rad/s$, and the damping factor is very low $\xi = 0.013$, we obtain the RLC filter values:

$$R=0.15\Omega,\ L=5mH,\ C=167\mu F$$

The calculation of voltage and current supported by the power switches is:

$$I_{SW} \geq I_{dc} = 3KA,\quad V_{SW} \geq 21.5KV$$

The controller parameters $R_i(p)$ are:

$$\tau_I = 50.01\mu s,\ \tau_d=16.66ms,\ K_p = 35,\ \tau=100\mu s$$

5.2 Sizing VSI_STATCOM parameters

The ripple level of the injected currents $\delta I_{inj}(\%)=10$. The value of the filter inductor is:

$$L'=41{,}31mH \text{ with } (R'=0{,}8\Omega)$$

The calculation of voltage and current supported by the power switches is:

$$I_{SW} \geq 2.17KA,\quad V_{SW} \geq V_{dc} = 90KV$$

The controller parameters $R_i'(p)$ are:

$$\tau'_I = 51.66ms,\ K' = 60$$

5.3 Simulation

The simulation is performed on the MATLAB / Simulink blocks using simulink and simpowersys libraries. The current unbalance factor **Ti** and the total harmonic current distortion **THD**, for the three-phase current in the power grid connection point are in functions of daily railway traffic. The **Ti**, and **THD** obtained by both structures are presented in the following figures:

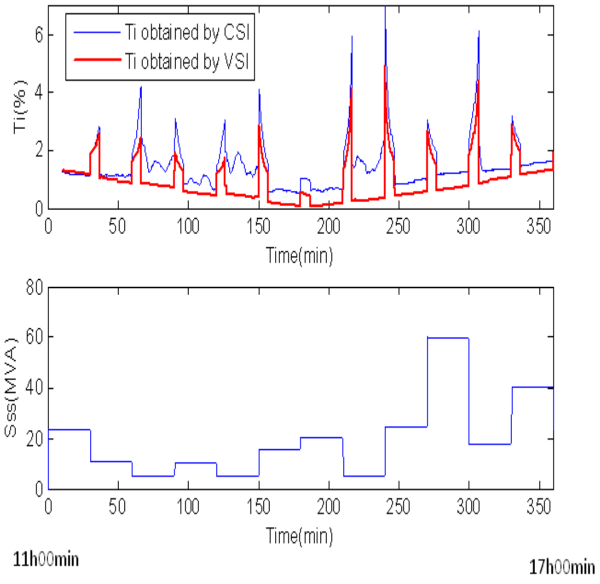

"**Figure 10:** Current unbalance factor Ti (%)."

IJERT

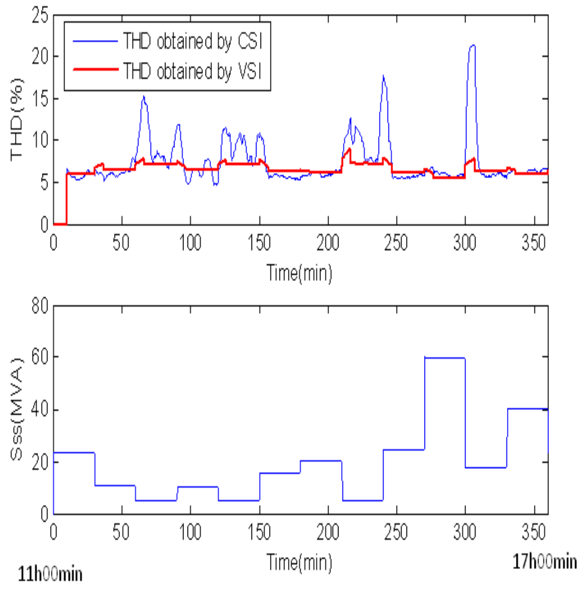

“**Figure 11:** Total harmonic current distortion THD (%).”

5.4 Comparison and results interpretation

- In the paragraphs (5.1) and (5.2), the calculation of the voltage and current supported by the switches shows that, the CSI structure is optimum in sizing terms (ie reduction of cost), because the voltage supported by the switch V_{sw} in the CSI case is reduced of **76%**. The following table summarizes the values found for V_{sw} and I_{sw} :

IJERT

“**Table 1**. The voltage and current value supported by the power switches”

	V_{sw}	I_{sw}
CSI Structure	21.5KV	3 KA
VSI Structure	90KV	2.17KA

- The figures (10) and (11) show that, for each change of power consumption level, we note that, an exceeding of the Ti and the THD, during transient regime. This exceeding is due to the response time of the injected current control loop. The VSI structure provides an exceeding reduced compared to the CSI structure.

- The exceeding of current unbalance factor and total harmonic current distortion obtain by CSI, is due to oscillations introduced by the RLC filter, because its natural pulsation chosen is not very much greater than that of the power grid (**ω_0=3.5*ω_r**) and its damping factor is low (**ζ = 0.013**). But if **ω_0** increases too much, filtering quality decreases and the **THD** exceeds the standard value.

- In the transient regime, the both structures (VSI and CSI) allow to control the current unbalance factor and the total harmonic current distortion in the standards (**Ti≤2% THD≤8%**). But the VSI structure allows to obtain a current unbalance factor more stable and lower than that obtained by the CSI structure

6. Conclusion

In this paper, a comparative study between both structures (VSI and CSI) of a shunt STATCOM used for current unbalance compensation caused by the sub-stations a high-speed railway was presented. The application of this study about the future sub-station planned for the high speed railway Tanger-Kenitra in Morocco, shows that the CSI structure is optimal in sizing terms, because it allows to have a switch voltage reduction of **76%**. The results obtained in the simulation of this application, shows that the control loop of the injected current for both structures allows to have, a current unbalance factor and total harmonic current distortion in the standards, but a VSI structure gives a **Ti** and **THD** more stable compared to the CSI structure.

7. References

[1] Gang Y., Lixue T., Lidan Z., and Chen C., “State-feedback Control of a Current Source Inverter-based STATCOM”. Electronics and Electrical Engineering Journal. 2010, N°3(99), 2010, pp. 17-22.

[2] Benslimane, A., Bouchnaif, J., Azizi, M., and Grari, K.,” Study of a STATCOM used for unbalanced current compensation caused by a high speed railway (HSR) sub-station”, Renewable and Sustainable Energy Conference. IRSEC’13, IEEE International. Ouarzazate, Morocco, 7-9 March 2013, pp. 441 – 446.

[3] Labrique, F., Seguier, G., and Bausiere, R., Les convertisseurs de l’éléctronique de puissance (la converstion continu-alternatif). book. Vol 4, 2nd Edition. Technique & Documentation-Lavoisier, 1995.

[4] Shen, D. and Lehn, P.W, “Modeling, Analysis, and Control of a Current Source Inverter-Based STATCOM”, IEEE Transactions on Power Delivery, vol. 17, n°1, , january 2002, pp 248-253.

[5] Ajami, A., and Younesi, M.,” Modeling and State Feedback Controller for Current Source Inverter Based

STATCOM”, Control, Automation and Systems Conference. ICCAS’08, IEEE International. Seoul, Korea, 14-17 October 2008, pp. 2418-2423.

[6] Wang, M.X, Pouliquen, H., and Grandpierro, M.,” Performance of an active filter using PWM current source inverter”, Power Electronics and Applications Fifth European Conference. IEEE International. Brighton, UK, 13-16 September 1993, pp. 218 - 223.

[7] Benslimane, A., Bouchnaif, J., Azizi, M.,” Etude des solutions de compensation du déséquilibre triphasé généré par les lignes d’alimentation des trains TVG dans le réseau THT”. Revue Enseigner l'Electrotechnique et l'Electronique Industrielle, N°70, octobre 2012, pp 64-70.

IJERT